Earth and Planetary Science Letters 361 (2013) 379–390

Contents lists available at SciVerse ScienceDirect

Earth and Planetary Science Letters

journal homepage: www.elsevier.com/locate/epsl

Volatile-rich silicate melts from Oldoinyo Lengai volcano (Tanzania): Implications for carbonatite genesis and eruptive behavior

J. Maarten de Moor [a,*], Tobias P. Fischer [a], Penelope L. King [b,c], Roman E. Botcharnikov [d], Richard L. Hervig [e], David R. Hilton [f], Peter H. Barry [f], Frederick Mangasini [g], Carlos Ramirez [h]

[a] Department of Earth and Planetary Sciences, University of New Mexico, Albuquerque, NM 87131, USA
[b] Institute of Meteoritics, University of New Mexico, Albuquerque, NM 87131, USA
[c] Research School of Earth Sciences, Australian National University, Canberra ACT 0200, Australia
[d] Institut für Mineralogie, Callinstr. 3, Leibniz Universität Hannover 30167, Hannover, Germany
[e] School of Earth and Space Exploration, Arizona State University, Box 871404, Tempe, AZ 85287, USA
[f] Scripps Institution of Oceanography, University of California San Diego, CA 92093 0244, USA
[g] Department of Mining and Mineral Processing Engineering, University of Dar Es Salaam, Tanzania
[h] Centro de Investigaciones Geofisicas, University of Costa Rica, San Jose, Costa Rica

ARTICLE INFO

Article history:
Received 21 May 2012
Received in revised form
17 October 2012
Accepted 2 November 2012
Editor: T. Elliot
Available online 20 December 2012

Keywords:
Oldoinyo Lengai
volatiles
explosive eruption
liquid immiscibility
mantle source

ABSTRACT

This study presents volatile, trace, and major element compositions of silicate glasses (nepheline-hosted melt inclusions and matrix glass) from the 2007–2008 explosive eruption at Oldoinyo Lengai volcano, Tanzania. The bulk compositions of the heterogeneous ash erupted in 2007–2008 are consistent with physical mixing between juvenile nephelinite magma and natrocarbonatite emplaced during the preceding ~25 years of effusive carbonatite eruption. The melt inclusions and matrix glasses span a wide range of silica-undersaturated compositions, from ~46 wt% SiO_2 and (Na+K)/Al~3 in the least evolved melt inclusions to 38 wt% SiO_2 and (Na+K)/Al up to 12 in the matrix glass. The depletion in SiO_2 between melt inclusions and matrix glass is accompanied by strong enrichment in all of the incompatible trace elements measured (Ba, Nb, La, Ce, Sr, Zr, Y), which is consistent with fractional crystallization of a bulk mineral assemblage with SiO_2 higher than that of the melt inclusions but inconsistent with silicate melt evolution by assimilation of carbonatite. The melt inclusions are volatile-rich with 2.7 wt% to 8.7 wt% CO_2 and 0.7 wt% to 10.1 wt% H_2O, indicating that Oldoinyo Lengai is a hydrous system. This is contrary to the long-held assumption that Oldoinyo Lengai is relatively anhydrous, which is based on the observation that natrocarbonatite lavas are water-poor. We argue that natrocarbonatites are derived from hydrous carbonate liquid that degas H_2O at low pressure. The silicate glass data show that H_2O concentration is negatively correlated with incompatible element enrichment, which we attribute to crystallization of the melt in response to decompression degassing of H_2O. The eruptive cycle at Oldoinyo Lengai reflects changes in bulk silicate magma viscosity due to extensive H_2O-driven crystallization and explosive eruptions occur when volatiles (i.e. $H_2O > CO_2$ gas, and carbonate liquid) cannot separate from the crystal-rich nephelinite magma. Melt H_2O content decreases as a function of pressure; however CO_2 concentration in the melt inclusions is buffered by the presence of immiscible carbonate liquid. CO_2 content increases with melt evolution parameters (e.g. increasing (Na+K)/Al) due to enhanced solubility with alkali enrichment and SiO_2 depletion in the melt. The matrix glasses and evolved melt inclusions, on the other hand, experienced low pressure (< 50 MPa) CO_2 degassing and were not buffered by a coexisting carbonate liquid. Whereas the melt inclusions are the most CO_2-rich yet identified, their CO_2/Nb ratios are without exception lower than that in MORB, indicating that a volatile-rich mantle source is not required for Oldoinyo Lengai.

1. Introduction

Oldoinyo Lengai (OL) is the only active carbonatite volcano worldwide and has played a pivotal role in the field of carbonatite petrogenesis. Silicate magmatic products are however the volumetrically dominant component of the magma system (e.g. Klaudius and Keller, 2006) and are amongst the most peralkaline

* Corresponding author. Tel.: +1 505 506 0264.
E-mail addresses: mdemoor@unm.edu (J.M. de Moor), fischer@unm.edu (T.P. Fischer), penny.king@anu.edu.au (P.L. King), r.botcharnikov@mineralogie.uni-hannover.de (R.E. Botcharnikov), richard.hervig@asu.edu (R.L. Hervig), drhilton@ucsd.edu (D.R. Hilton), pbarry@ucsd.edu (P.H. Barry), mangatz@yahoo.co.uk (F. Mangasini), carlosjru@yahoo.com (C. Ramirez).

0012-821X/$ - see front matter © 2012 Elsevier B.V. All rights reserved.
http://dx.doi.org/10.1016/j.epsl.2012.11.006

silica undersaturated compositions known (e.g. Mitchell and Dawson, 2012). As such, OL represents an important endmember magmatic system in terms of terrestrial volcanism and presents a unique opportunity to investigate volatile behavior in an active peralkaline silicate–carbonatite system.

Carbonatites are in themselves a diverse group of magmatic products (e.g. Mitchell, 2005), and the natrocarbonatites erupted at OL are alkali-rich. However, it is increasingly recognized that carbonatite inclusions from many carbonatite-silicate magmatic complexes are rich in alkalis and may be akin to natrocarbonatites (e.g. Guzmics et al., 2011; Nielsen et al., 1997; Sokolov et al., 1999). Kimberlites may originate as carbonatite-like melts in the mantle (e.g. Safonov et al., 2011; Wyllie and Huang, 1975) in order to carry sufficient volatiles to erupt explosively from depth (e.g. Brooker et al., 2011; Russell et al., 2012). The role of volatiles, particularly CO_2 and H_2O, is fundamental to the genesis and eruption of carbonatites and kimberlites, yet direct analyses of volatiles in highly undersaturated natural melts are lacking. As OL is the only active carbonatite volcano on Earth, its magmatic system provides important insights into the genesis of carbonatites and their relationship to undersaturated silicate magmas.

The close association between carbonatites and alkali-rich silica-undersaturated nephelinite and phonolite magmas is exemplified by the eruptive cycle at OL, where extended periods of natrocarbonatite effusion are punctuated by explosive ash eruptions dominated by nephelinitic products. The 2007–2008 explosive eruption was bracketed by natrocarbonatite effusion, and study of the ash deposits has sparked renewed debate on the magmatic system and particularly on the role of volatiles in generating explosive eruptions at OL. Here we present analyses of CO_2, H_2O, and trace elements in silicate melt inclusions from OL to investigate (1) the behavior of volatiles in highly alkaline silicate melts associated with carbonatites; (2) the role of volatiles in the 2007–2008 eruption; and (3) volatile characteristics of the OL mantle source.

1.1. 2007–2008 Explosive eruption of Oldoinyo Lengai

In September 2007, OL experienced an explosive eruption that lasted until July of 2008, producing ash columns up to 15 km high and forming a pit crater >100 m deep (Kervyn et al., 2010). Natrocarbonatite effusion from 1983–2007 preceded the explosive eruption (Kervyn et al., 2010). We observed extremely low-viscosity lava (a diagnostic attribute of natrocarbonatite, though no samples are available for confirmation) at the bottom of the pit crater in July 2009. This cycle of prolonged natrocarbonatite effusion and violent nephelinitic eruptions typifies the eruptive behavior of OL (e.g. Dawson et al., 1995; Keller et al., 2010).

The 2007–2008 explosive eruption first produced mixed natrocarbonatite+nephelinite ash and later produced dominantly combeite–wollastonite nephelinite ash (Keller et al., 2010, Mattsson and Reusser, 2010). Keller et al. (2010) considered the natrocarbonatite+nephelinite ash to be a new hybrid magma type close to immiscible separation into two conjugate liquids, whereas Mitchell and Dawson (2007) considered the natrocarbonatite+nephelinite ash to be a physical mixture of two distinct magma reservoirs. Mitchell (2009) reported the occurrence of nepheline-hosted melt inclusions consisting of quenched immiscible silicate and carbonate liquids in the 2007–2008 products, providing the most robust physical evidence for genesis of natrocarbonatite by liquid immiscibility. We follow the terminology of Webster and Mandeville (2007) when referring to melts, liquids, fluids, and vapors in the complex multicomponent system of OL and a brief review of the definitions of these terms is given in the Supplementary Material.

2. Samples and analytical methods

2.1. Samples

The lapilli and ash deposits from the 2007–2008 eruption contain abundant crystals, xenolithic material ($>30\%$ in some deposits), a variable component of natrocarbonatite, and juvenile crystal-rich vesicular scoriae (Fig. 1a and b). Our samples are from two scoria-rich layers from a 0.51 m thick ash sequence on the west slope of the volcano (S2°45.40′; E35°54.44′) collected in April 2008 during explosive activity and from a 0.85 m thick stratigraphic sequence in the inactive south crater (S2°45.88′; E35°55.04′) collected in July 2009. The samples used in this study are from two layers containing the highest proportions of juvenile lapilli and are coarse grained, relatively equigranular and were probably deposited from the paroxysmal nephelinitic eruptions in early 2008 (eruption columns >10 km; Kervyn et al., 2010). Vesicular scoriae are phenocryst-rich (usually $>50\%$), and contain nepheline, clinopyroxene, garnet, wollastonite, apatite $\pm$ combeite, $\pm$ melilite, $\pm$ sulfides (Fig. 1b; Keller et al., 2010; Mitchell, 2009; Mitchell and Dawson, 2007). The matrices of the scoriae are microlite-rich with interstitial glass.

We report compositions of melt inclusions trapped in nepheline crystals and matrix glass in vesicular lapilli representing melt compositions in the pre-eruptive magma chamber and residual melt quenched at eruption, respectively. Analysis of glasses avoids problems associated with whole rock analysis of these highly heterogeneous mixed pyroclastic deposits and provides information on the compositions of the silicate melts responsible for the explosive eruption and associated with natrocarbonatite lavas at OL.

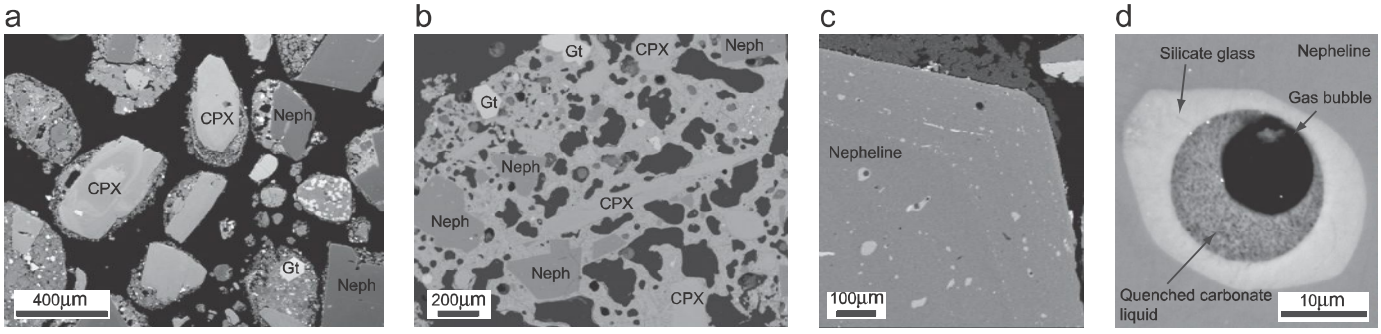

Fig. 1. BSE images of (a) ash with a variety of clasts including carbonate-mantled lapilli, ijolite xenoliths and juvenile lapilli, (b) vesicular, phenocryst- and microlite-rich lapillus containing nepheline, clinopyroxene, and garnet as phenocryst phases. Wollastonite and combeite occur as microphenocrysts, (c) euhedral nepheline crystal with zoned melt inclusions and (d) three-phase inclusion with silicate glass coexisting with quenched carbonate liquid and a vapor bubble.

We targeted round to oval, glassy, homogenous silicate melt inclusions free of daughter crystals. Some of the inclusions contain a quenched carbonate globule+vapor bubble coexisting with the silicate glass (Fig. 1d), similar to those that were described by Mitchell (2009) and Mitchell and Dawson (2012). The proportion of silicate glass to carbonate is highly variable, similar to those reported by Sharygin et al. (2012) who provided detailed descriptions of multi-phase inclusions from a c. 1917 OL lava flow. The carbonate component is composed of finely crystalline quench material (Fig. 1d) and is considered to represent a carbonate liquid that is parental to the natrocarbonatite lavas erupted to the surface (Mitchell, 2009).

2.2. Analytical methods

Melt inclusions and matrix glasses were analyzed on a JEOL 8200 electron microprobe at the University of New Mexico for major and minor elements, and on a Cameca ims 6F secondary ion mass spectrometer (SIMS) at Arizona State University for CO_2, H_2O, and trace elements. Matrix-matched standards for SIMS analysis of CO_2 and H_2O were prepared at temperatures between 1000 °C and 1200 °C and pressures between 110 MPa and 500 MPa in an Internally Heated Pressure Vessel (IHPV) at Leibniz Universität Hannover. The standard glasses were analyzed by ELTRA CS analyzer and Karl-Fischer titration for bulk CO_2 and H_2O contents, respectively, at Leibniz Universität Hannover. The details of standard preparation, analytical methods, and calibration curves used for SIMS analysis of CO_2 and H_2O are presented in the Supplementary Material. All samples and standards were polished for microanalysis using kerosene and were stored in dessicators at all times. An assessment of possible glass contamination (Supplementary Material) reveals that these glass compositions are not affected by atmospheric absorption during the sample preparation methods used in this work. A separate study on calibration of various analytical techniques for measurement of volatiles in these extreme glass compositions is in progress.

3. Results

3.1. Major elements

Compositions of matrix glass and melt inclusions are reported in the supplementary material (Tables A3 and A4, respectively) and representative compositions are presented in Table 1. Fig. 2 shows molar (Na+K)/Al versus SiO_2 for melt inclusions and matrix glasses compared to whole rock and glass compositions reported in previous studies (Keller et al., 2010; Klaudius and Keller, 2006; Mattson and Reusser, 2012; Mitchell, 2009; Mitchell and Dawson, 2012). The glasses span a large range in composition and define a cohesive evolutionary trend of decreasing SiO_2 from ~46 wt% in melt inclusions to ~38 wt% in matrix glass, though considerable overlap exists. Our data are consistent with compositions reported in previous studies (Fig. 2), and show that the glasses from the 2007–2008 eruption show depletion of SiO_2 (i.e. from melt inclusions to matrix glass), which is accompanied by strong enrichment in Na_2O (13.8–21 wt%), FeO (8.8–15.1 wt%), MnO (0.3–0.8 wt%), CaO (3.3–8.7 wt%), P_2O_5 (0.1–0.9 wt%), S (0.3–1.2 wt%), F (0.2–0.9 wt%), and Cl (0.3–0.6 wt%). All of the glasses are poor in MgO (0.4–1.4 wt%). Al_2O_3 is the only oxide other than SiO_2 to show a clear depletion trend (10.8–3.6 wt%) between melt inclusions and matrix glass whereas K_2O (6.9–4.8 wt%) shows weak correlation with SiO_2. Melt inclusions near nepheline rims overlap with compositions of matrix glass, whereas those closer to the center of nepheline crystals have higher SiO_2 and Al_2O_3 and lower Na_2O, indicating that the melt evolved along the trend defined in Fig. 2 throughout growth of nepheline phenocrysts in the magma chamber.

Table 1
Major, volatile, and trace element compositions of representative nepheline-hosted melt inclusions, as well as the average composition of matrix glass (n=63 for major element, n=15 for CO_2 and H_2O, and n=8 for trace elements). Major and volatile element concentrations are in wt% and trace element concentrations are in ppm.

	Less evolved melt inclusion	Melt inclusion with immiscible carbonate	Evolved melt inclusion	Average matrix glass
Analysis ID	Neph3_3	E-34_4	Neph11_5	
SiO_2	47.98	41.57	40.01	40.66
TiO_2	0.65	1.75	2.14	1.41
Al_2O_3	10.55	8.25	4.33	4.66
FeO_T	8.34	11.40	12.65	14.14
MnO	0.23	0.57	0.72	0.70
MgO	0.37	1.11	1.29	1.11
CaO	3.80	4.19	7.62	7.41
Na_2O	13.62	15.64	18.24	19.26
K_2O	6.23	6.01	5.03	5.70
P_2O_5	0.11	0.38	0.71	0.61
S	0.32	0.47	0.74	0.88
Cl	0.26	0.42	0.47	0.49
F	0.25	0.28	0.59	0.59
H_2O	5.59	5.46	1.62	0.66
CO_2	2.76	3.27	6.83	3.09
−O=S,Cl,F	−0.32	-0.45	−0.72	−0.80
Total	100.73	100.30	102.26	100.59
(Na+K)/Al	2.76	3.91	8.18	8.12
Ba	1260	2210	5870	6439
Sr	1136	1783	4651	5246
Zr	376	751	1474	1762
Nb	118.3	263.8	609.2	627.6
La	34.5	222.3	538.4	546.5
Ce	49.1	334.1	764.7	830.5
Y	13.4	49.9	59.3	68.2

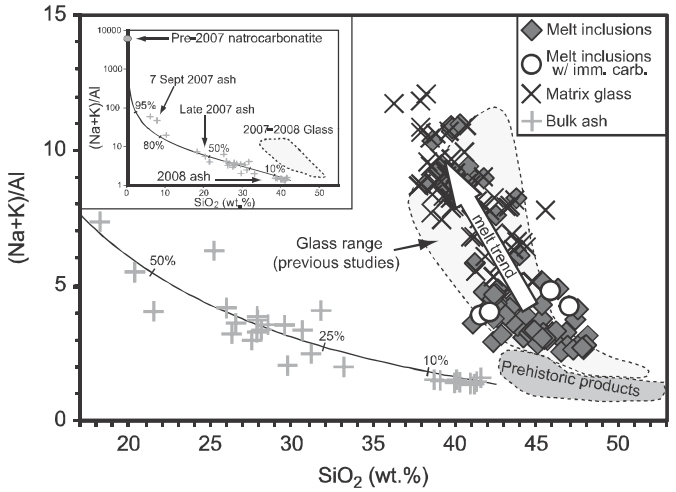

Fig. 2. Molar (Na+K)Al versus SiO_2 showing compositions of the silicate glasses (melt inclusions, melt inclusions containing an immiscible carbonate phase, and matrix glass) from the 2007–2008 explosive eruption. Silicate glass data from previous studies (Mitchell, 2009; Mitchell and Dawson, 2012) are shown as a light grey field. Whole rock compositions (Keller et al., 2010; Mattsson and Reusser, 2010; Mitchell and Dawson, 2007; this study) are well described as a physical mixture between 1988–2007 average natrocarbonatite (Keller et al., 2010) and the silicate endmember (i.e. juvenile nephelinite+ijolite xenoliths) erupted in mid 2008. The field for "Prehistoric products" shows the whole rock data range for nephelinitic and phonolitic products from Klaudius and Keller (2006). Mixing line is shown as a solid curve and the inset shows that the eruption progressed from natrocarbonatite-rich to natrocarbonatite-poor (whole rock data from Keller et al., 2010, Mattsson and Reusser (2010), Mitchell and Dawson (2007), and this study).

3.2. Trace elements

SIMS analyses (Tables A5 and A6) show that matrix glasses are enriched in incompatible elements relative to melt inclusions. La

and Ce are enriched in matrix glass by up to a factor of ~20 relative to melt inclusions (total range; La 49–880 ppm; Ce 59–1263 ppm). Yttrium is enriched in matrix glass relative to the least evolved melt inclusions by up to a factor of ~7 (13–93 ppm). The high field strength elements Nb (118–771 ppm) and Zr (367–2172 ppm) are enriched by up to a factor of ~6, whereas the large ion lithophile elements Ba (1020–9551 ppm) and Sr (907–8267 ppm) are enriched by up to a factor of ~9. The trace element abundances reported here span the range in concentrations reported by Sharygin et al. (2012) for nepheline-hosted melt inclusions from a nephelinite lava flow erupted in ~1917. Their inclusions have a narrower range in trace element concentrations and are comparable to the most enriched samples from this study.

3.3. CO_2 and H_2O

Fig. 3 shows that melt inclusions have a wide range in H_2O contents, that CO_2 concentration increases with decreasing H_2O in melt inclusions, and that matrix glasses attain low H_2O and CO_2. Melt inclusions contain 2.7–8.7 wt% CO_2, representing the most CO_2-rich natural silicate glasses reported to date by over an order of magnitude (Vigouroux et al., 2008). Water concentrations vary between 0.7 wt% and 10.1 wt%, indicating that the OL magma system is hydrous, which is in contrast to previous assumption that the magma system is anhydrous (e.g. Keller et al., 2010; Mitchell and Dawson, 2012). The matrix glasses contain <0.1 wt% to 7.1 wt% CO_2 and <0.1 wt% to 3.1 wt% H_2O. The least evolved melt inclusions (i.e. those with lowest incompatible element concentrations) contain up to 10.1 wt% H_2O and ~1 wt% CO_2. Melt inclusions show decreasing H_2O (to ~1 wt%) and increasing CO_2 (to 8.7 wt%) with increasing trace element concentrations and decreasing SiO_2. Sharygin et al. (2012) reported low water contents (0.1–0.6 wt% H_2O, although their analyses were calibrated using an sub-optimal standard that is not matrix matched) in melt inclusions from the ~1917 lava flow, consistent with the trace element enriched nature of those glasses. Silicate melt inclusions with a coexisting quenched carbonate liquid (usually with coexisting vapor bubble; Fig. 1(d)) occur over the range in CO_2 and H_2O observed in melt inclusions. Matrix glass has a distinct trend from the melt inclusions and is depleted in H_2O relative to the most evolved inclusions, and shows a broad range in CO_2 content extending to depleted concentrations (<0.1 wt% CO_2).

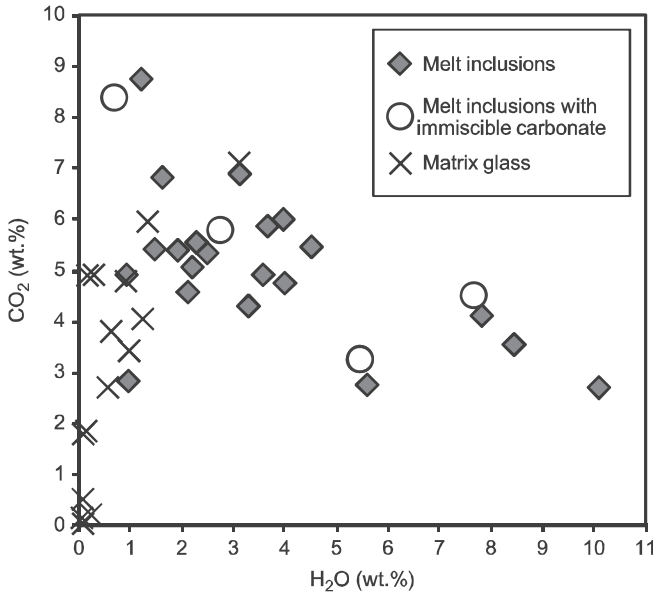

Fig. 3. Plot of CO_2 versus H_2O showing compositions of melt inclusions and matrix glass. Inclusions containing immiscible carbonate (Fig. 1d) span the range of CO_2 and H_2O contents observed in the melt inclusions.

4. Discussion

We consider three hypotheses in the interpretation of melt inclusion and matrix glass compositions: (1) The silicate melt may be controlled by equilibration with a coexisting carbonate liquid (Section 4.1); (2) The compositional variation between melt inclusions and matrix glass may reflect assimilation of natrocarbonatite, as proposed by Mitchell and Dawson (2007, 2012) (Section 4.2); (3) Degassing and fractional crystallization may control the observed evolutionary trends (Fig. 2) (Section 4.3).

4.1. Silicate melt evolution in the presence of carbonate liquid

Fig. 4 shows a quasi-ternary plot (projected from CO_2; see Brooker and Kjarsgaard (2011) for a thorough review of SiO_2–NaO–Al_2O_3–CaO–CO_2 (SNAC) diagrams) of silicate glass compositions from the 2007–2008 eruption. Also shown are the average composition of quenched carbonate inclusions (that coexist with silicate glass) hosted in nephelines from the same eruption (Mitchell, 2009), fields for other silicate magmas occurring in carbonatite complexes (Brooker and Kjarsgaard, 2011), and solvi for two immiscible liquid compositions (solid lines). The silicate melt inclusions fall close to the 100 MPa, 700 °C solvus determined experimentally by Kjarsgaard et al. (1995) using natural OL nephelinite and natrocarbonatite compositions, and overlap with the silicate glass compositions reported by Mitchell (2009) (Fig. 2). The quenched carbonate inclusions lie on the silica-poor limb of the solvus, consistent with carbonate liquid immiscibility with the silicate melt.

The width of the two liquid solvus decreases with decreasing pressure, increasing temperature, decreasing alkali content and decreasing partial pressure of CO_2 (PCO_2; see Brooker and Kjarsgaard (2011) for a full discussion of phase relations in immiscible silicate–carbonate systems). Matrix glasses from the 2007–2008 eruption plot at more silica-depleted and alkali-rich compositions than melt inclusions, as previously observed in Fig. 2, on a trajectory towards the quenched carbonate liquid composition (SI–CL line). This could be interpreted to reflect equilibrium contraction of the two liquid field due to decrease in total pressure and/or PCO_2 (e.g. by dilution with another volatile component; Brooker and Kjarsgaard, 2011). Increasing temperature or decreasing alkali content of the bulk system could have a similar effect. However, these latter suggestions are rejected as plausible explanations because no textural evidence exists for massive reheating of the system, and alkalis are enriched in matrix glass (Fig. 2).

Fig. 4(inset) suggests that the peralkalinity of the silicate melt is buffered at 4–5 by the presence of an immiscible carbonate liquid at variable and high CO_2 content, as reflected by the melt inclusions with coexisting carbonate liquid. In the least evolved melt inclusions ($(Na+K)/Al<6$), CO_2 content increases with increasing alkalis and decreasing SiO_2, which is interpreted to reflect increasing CO_2 solubility due to depolymerization of the melt as Na^+ is enriched and SiO_2 is depleted (Fig. 2). The matrix glasses (which do not have coexisting carbonate globules in our samples) and a population of carbonate-free melt inclusions attain high peralkalinity and highly variable CO_2 contents, from ~6 wt% to degassed compositions of <0.5 wt%. We interpret these trends to reflect melt evolution and CO_2 degassing with no

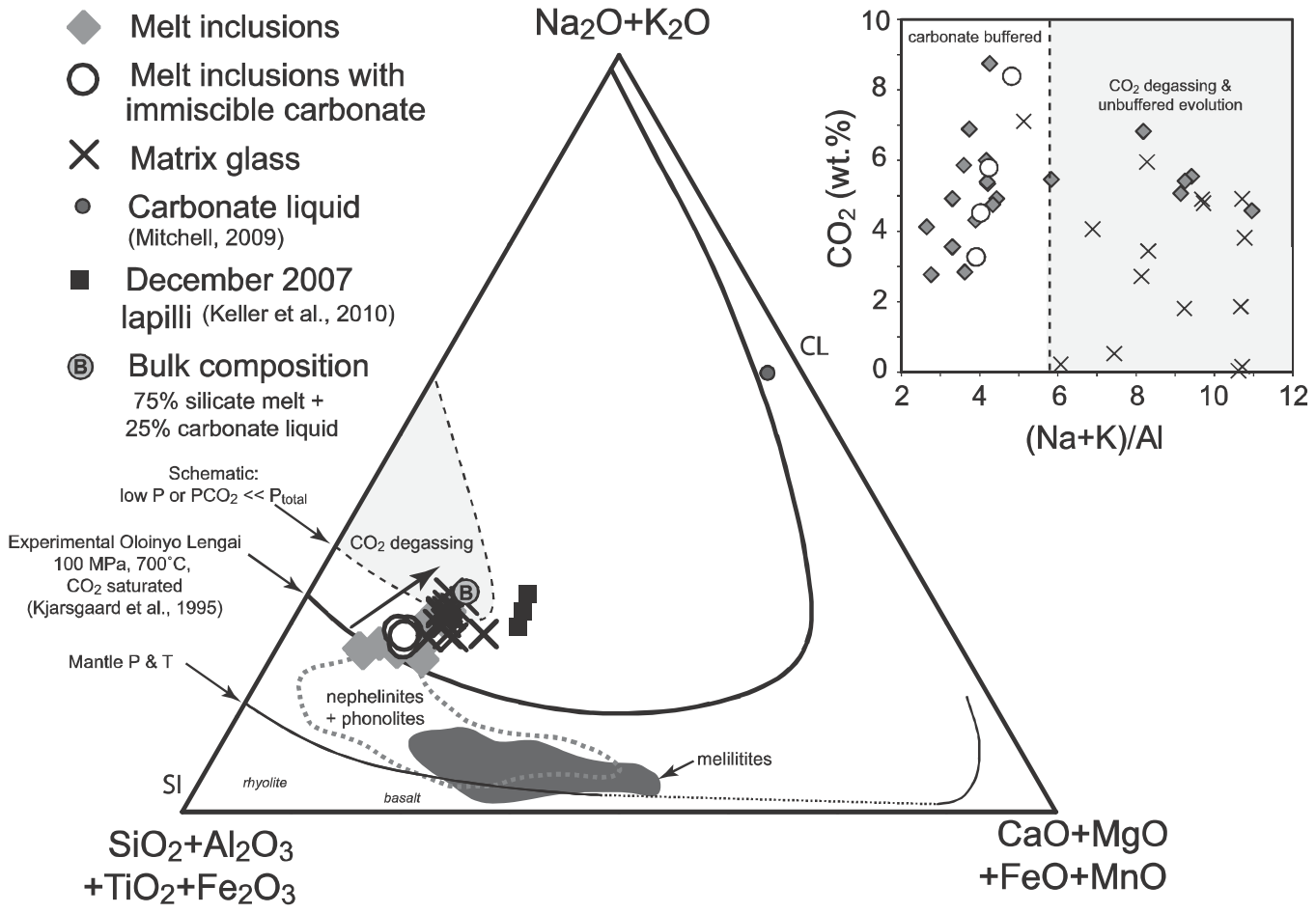

Fig. 4. Quasi-ternary plot projected from CO_2 (after Brooker and Kjarsgaard, 2011 see their Fig. 11) showing compositions of silicate melt inclusions, silicate melt inclusions that contain an immiscible carbonate phase, and matrix glass from the 2007–2008 eruptive products. Also shown are the compositions of the immiscible quenched carbonate liquid from multi-phase inclusions reported by Mitchell (2009). Fields for alkali silicate rocks found in carbonatite complexes and experimentally determined two-liquid solvi for mantle and OL conditions are also shown (Brooker and Kjarsgaard, 2011). The two-liquid solvus contracts with decreasing pressure, decreasing alkali content, decreasing pCO_2, and increasing temperature. However, pressure is the dominant control. The point marked "B" refers to the composition of the bulk system (i.e. silicate melt+carbonate liquid), and was calculated using a mixing ratio of 75% silicate melt (from compositions of silicate melt inclusions with immiscible carbonate) and 25% carbonate liquid (from compositions of carbonate liquid reported by Mitchell, 2009), which is the carbonate-rich end of the spectrum for estimates of the bulk silicate–carbonate system (2% to 25% carbonate; Kjarsgaard et al., 1995; Pyle et al., 1991; Williams et al., 1986). A more conservative estimation of the bulk composition would lie closer to the silicate "melt inclusions with immiscible carbonate" compositions. The line SI–CL is the trace of the projection plane used in Fig. 7. The "CO_2 degassing" field is shown schematically to correspond to low P conditions resulting in loss of CO_2 gas in the absence of carbonate liquid, as observed in the matrix glass compositions (inset; Fig. 4). The inset shows that CO_2 concentration increases with (Na+K)/Al at (Na+K)/Al < 6, which is interpreted to reflect carbonate-buffered conditions. Melt inclusions and matrix glass with (Na+K)/Al > 6 show a wide range in CO_2 content extending to degassed compositions, which is interpreted to reflect unbuffered conditions in response to decompression.

buffering by a carbonate liquid and depict this on the SNAC diagram with a dashed field: "CO_2 degassing".

4.2. Silicate melt evolution by assimilation of natrocarbonatite

Mitchell and Dawson (2007) proposed that the cause of the 2007–2008 explosive eruption was a decarbonation reaction resulting from natrocarbonatite assimilation by "high-temperature nephelinite magmas", producing CO_2 gas (that drove the explosivity) and highly peralkaline low SiO_2 silicate melt, essentially due to dilution by assimilated natrocarbonatite.

Trace elements provide an effective tool for assessing this assimilation hypothesis because the natrocarbonatite lavas and nephelinite magmas at OL have distinctive trace element compositions related to partitioning between carbonate liquids and silicate melts (Fig. 5a). Within our trace element dataset, Ba and Zr provide the most insight into potential assimilation of natrocarbonatite by the silicate melt because Ba partitions strongly into the natrocarbonatite magma ($C^{Ba}_{natrocarbonatite}/C^{Ba}_{nephelinite} \approx 10$), whereas Zr partitions strongly into the silicate melt ($C^{Zr}_{natrocarbonatite}/C^{Zr}_{nephelinite} \approx 0.01$) (Keller and Spettel, 1995; for experimental work also see: Hamilton et al., 1989; Kjarsgaard et al., 1995; Veksler et al., 1998). Fig. 5b shows a plot of Zr versus Ba for silicate melt inclusions, matrix glass, and recent natrocarbonatite lavas. Melt inclusions and matrix glasses show a cohesive trend with positive slope from melt inclusions to more evolved matrix glass. Natrocarbonatite lavas form a separate trend at low Zr concentrations and high Ba with negative slope. Shallow assimilation (i.e. late in the evolutionary history of the silicate magma) of previously emplaced natrocarbonatite by the silicate melt would result in decreased Zr (i.e. by dilution) accompanied by increased Ba in the matrix glass, which is not observed.

Similarly, Y and Nb are depleted in natrocarbonatites and enriched in nephelinites from OL, and the matrix glass shows enrichment of these elements relative to melt inclusions. Zirconium, Y, and Nb all increase with decreasing SiO_2, the opposite of

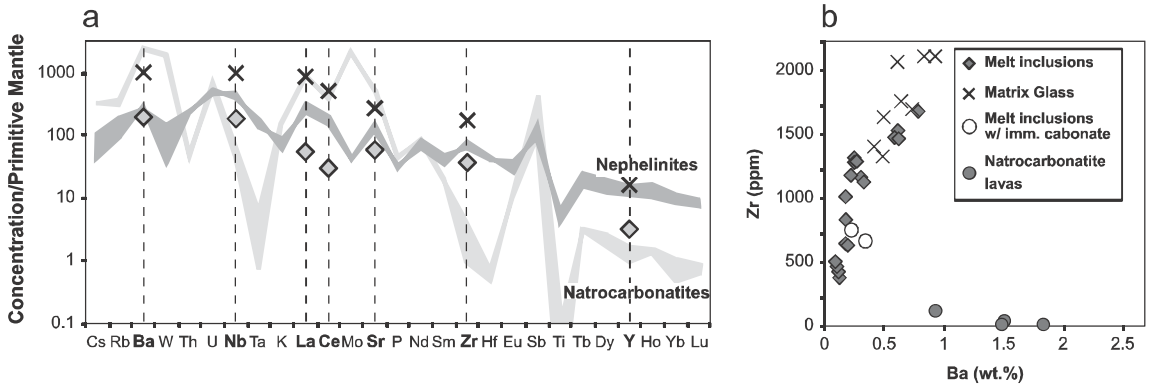

Fig. 5. (a) Incompatible element diagram showing that average matrix glass is enriched in all incompatible elements relative to melt inclusions (Neph3_3; from data reported in Table 1), which is consistent with evolution by fractional crystallization and inconsistent with assimilation of natrocarbonatite. Data for "Nephelinites" and "Natrocarbonatites" ranges are from Keller and Spettel (1995) and from bulk samples from the 2007–2008 deposits and from a fresh 2005 natrocarbonatite flow (this study). (b) Zr versus Ba showing the compositions of melt inclusions, matrix glass, and carbonatite lavas (from Keller and Spettel, 1995 and this study). The evolution from melt inclusions to matrix glass is inconsistent with assimilation of natrocarbonatite lava.

what would be expected if the depletion in SiO_2 was due to assimilation of silica-poor natrocarbonatite. Therefore, none of the expected trace element signatures associated with the proposed natrocarbonatite assimilation are observed, and the hypothesis of Mitchell and Dawson (2007) that the enrichment in alkalis and depletion in SiO_2 (Fig. 2) is due to assimilation of natrocarbonatite is rejected. Other arguments against assimilation as the cause of the explosive eruption are given in Keller et al. (2010) and Mattsson and Reusser (2010).

4.3. Crystallization of silicate melt

As with all other magma types, crystallization must play a fundamental role in the evolution of the OL silicate magmas, especially considering the crystal-rich nature of the 2007–2008 samples (Fig. 1b). The recent magmas from OL are highly evolved, as evidenced from their enriched trace element compositions (Keller et al., 2010; Klaudius and Keller, 2006). The diversity and heterogeneity of the eruptive products, even within the 2007–2008 ashes, speaks to the complexity of the magmatic system, with distinguishable sub categories of nephelinitic components present in the deposits (e.g. combeite–wollastonite nephelinite, mellilite-bearing nephelinite; Mitchell and Dawson, 2012).

The mineralogical diversity of the 2007–2008 eruptive products, the heterogeneity of the ashes, and the effects of carbonate liquid separation and extraction (Section 4.1) obscure a major-element based fractional crystallization assessment of the silicate melt evolution. In this regard, trace element compositions of glasses (i.e. from less enriched melt inclusions to highly enriched matrix glass) provide an alternative approach to assessing the role of crystallization in the silicate melt. The spatial resolution (~7 μm) of high-precision SIMS analysis of trace elements in melt inclusions and interstitial matrix glass provides unprecedented insight into melt evolution processes at OL. It is important to note that we only address the compositional variation within our dataset and do not attempt to establish a genetic relationship to a primitive parental source magma for the OL nephelinites.

The primary observation of the dataset presented here is that all of the incompatible trace elements are enriched in matrix glass relative to melt inclusions. Part of this enrichment must be due to crystallization because, considering the endmember scenario of carbonate liquid extraction with no crystallization, the silicate melt would be depleted in elements that are more compatible in the carbonate liquid. The light REE best exemplify trace elements that are strongly compatible in the carbonate liquid (Hamilton et al., 1989; Keller and Spettel, 1995) (Fig. 5b). La and Ce are enriched by a factor of ~20 between melt inclusions and matrix glass (considering the full compositional range), which is consistent with high degrees of crystallization and inconsistent with carbonate liquid extraction only. Furthermore, these elements are compatible in apatite (e.g. Watson and Green, 1981), a phase observed as a microphenocrysts/microlites and as inclusions in nepheline phenocrysts. Significant apatite crystallization would therefore also deplete the silicate melt in La and Ce. Crystallization of phases that do not incorporate the light REE (i.e. the primary nephelinite phenocryst phases: nepheline, clinopyroxene, and garnet) must therefore predominate as the process controlling La and Ce enrichment.

In Section 4.2 we showed that assimilation of natrocarbonatite is an insignificant factor in the compositional evolution of the silicate melt. The trace element enrichment cannot be attributed to assimilation because this process would result in dilution of trace elements (Y, Zr, Nb) that are depleted in the carbonate liquid during immiscible separation. We observe an enrichment by a factor of ~7 for Y and ~6 for Zr between melt inclusions and matrix glass (full data range), which is again consistent with crystallization of the silicate melt and inconsistent with natrocarbonatite assimilation. The observation that Y and Zr are less enriched than La and Ce is consistent with the compatibility of these element in OL garnet (Petibon, 1999), which is a primary sub-liquidus phase in all of the recent silicate magmas at OL, and also occurs as one of the primary components of ijolitic cumulate xenoliths that are common in the eruptive deposits. We therefore conclude that the strong and ubiquitous incompatible element enrichment in the matrix glass relative to melt inclusions can only be attributed to extensive crystallization, which is consistent with the crystal-rich nature of the juvenile nephelinite lapilli and ijolite cumulates (Fig. 1b). If crystallization is the process responsible for trace element enrichment and La and Ce are assumed to be completely incompatible, then 95% fractional crystallization can account for the observed enrichment. This is probably a conservative value because carbonate liquid extraction and apatite crystallization both occurred and these phases incorporate light REE. Robust modeling of the differentiation processes could quantify the relative importance of fractional crystallization versus carbonate liquid extraction in melt evolution but would require trace element data for the phenocryst phases present as well as for the quenched carbonate liquid phase. SIMS analysis of the carbonates would require development of matrix matched standards, which is beyond the scope of this study.

Dawson (1998) highlighted the "paradox" in establishing a simple fractional crystallization relationship between moderately

peralkaline wollastonite nephelinite ((Na+K)/Al=~1.5) and highly peralkaline combeite nephelinites ((Na+K)/Al up to ~15 in matrix glasses) because the matrix glasses have lower SiO_2 than whole rock samples. Melt inclusions in our dataset also show significantly higher SiO_2 than matrix glasses and the average SiO_2 content of melt inclusions with (Na+K)/Al < 4 is 44.9 wt% (i.e. at or below carbonate liquid buffered conditions, Section 4.1). Clinopyroxene, wollastonite, and combeite from nephelinites at OL have SiO_2 concentrations > 50 wt% (average values of 50.6 wt%, 51.3 wt%, and 50.3 wt%, respectively; data compiled from Dawson, 1998; Keller et al., 2006; Kjarsgaard et al., 1995; Klaudius and Keller, 2006; Mattsson and Reusser, 2010; Mitchell and Dawson, 2007). Crystallization of these phases from a melt with lower SiO_2 content would therefore deplete the melt in SiO_2, providing a reasonable explanation for the depletion in SiO_2 in matrix glass. Fig. 6a shows that matrix glass is enriched in Ce but depleted in SiO_2, consistent with crystallization of a bulk phenocryst assemblage with higher SiO_2 than the melt, resulting in matrix glass enriched in Ce but depleted in SiO_2.

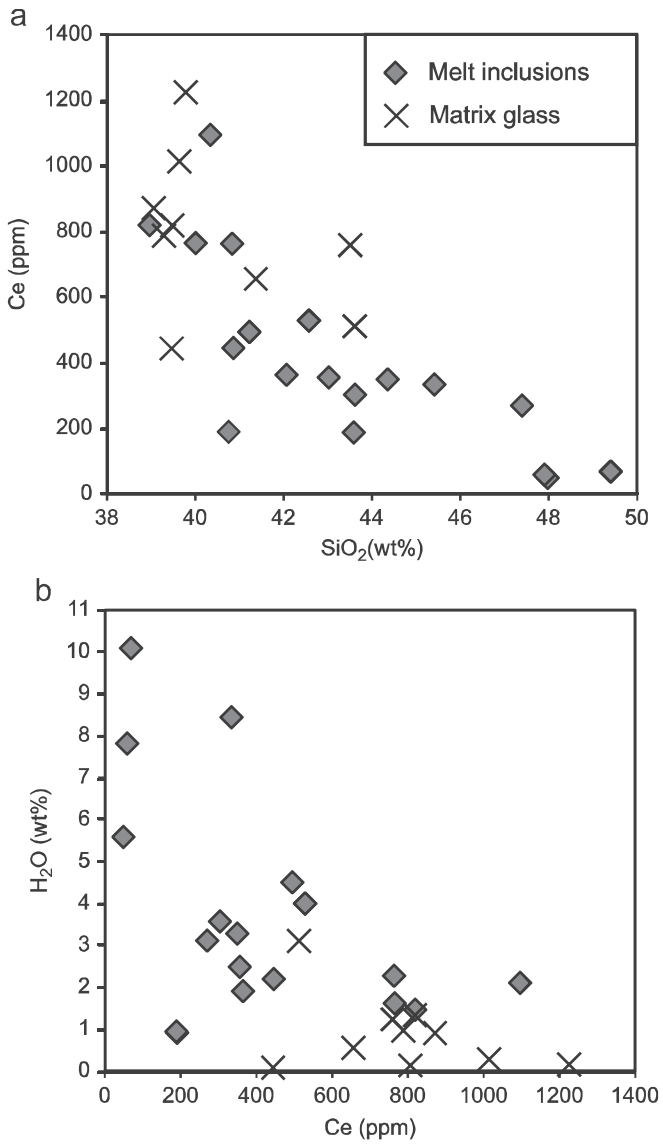

Fig. 6. (a) Plot a shows that Ce is enriched in the melt as SiO_2 is depleted, which is interpreted to reflect Ce enrichment by crystallization of a phenocryst assemblage with higher SiO_2 than the melt (see Section 4.3). (b) Plot b shows that H_2O degassing is associated with Ce enrichment, indicating that H_2O degassing drives crystallization.

4.4. The fundamental role of volatiles

4.4.1. Silicate melt evolution due to decompression and degassing

Fig. 6b shows that melt inclusions with the highest water contents are also the least evolved in terms of trace element enrichment due to differentiation. The correlation between H_2O loss and Ce enrichment, a trend that includes both melt inclusions and matrix glass, argues for a direct relationship between degassing of H_2O and crystallization (Fig. 6b), as is common for most silicate melts due to elevation of liquidus temperature with decreasing water content (e.g. Sparks, 2003).

We attribute the decrease in silicate melt H_2O concentration (Figs. 3 and 6b) to decompression degassing as the silicate magma ascended through the crust. A minimum estimate of melt inclusion entrapment pressure can be determined by considering the H_2O contents of melt inclusions. This is a minimum estimate because CO_2 content is not considered but exsolution of other gases (e.g. CO_2) may decrease H_2O fugacity and hence lead to fluid saturation at higher pressure. CO_2 and H_2O solubilities have not been determined for the compositions of OL silicate melts, and the high alkali contents of these melts could drastically alter their pressure dependences (e.g. Behrens et al., 2009; King and Holloway, 2002; Moore, 2008). Application of any CO_2–H_2O solubility model could therefore be misleading. Nevertheless, for the majority of melt inclusions containing 2 to 8 wt% H_2O, the H_2O solubility model for phonolite of Schmidt and Behrens (2008) gives pressure estimates between 30 and 300 MPa, which is generally compatible with previous estimates of magma chamber pressures at OL (e.g. Kjarsgaard et al., 1995; Petibon et al., 1998). As argued above, H_2O degassing plays a fundamental role in crystallization due to raising the temperature of the liquidus and solidus, which results in evolution of the silicate melt to more enriched compositions (Fig. 6b).

The unusual behavior of CO_2 in the OL silicate melt (Fig. 3) is more complex due to the buffering effect of a coexisting carbonate liquid (Fig. 4, projected from CO_2). Fig. 7a shows phase relations and the two liquid solvus in isobaric CO_2 space (after Brooker and Kjarsgaard, 2011) along the line SI–CL in Fig. 4, which is defined by the compositions of the coexisting silicate and carbonate liquids and projected to the axes. The bulk composition (point "B") is shown schematically along the tie line between the silicate melt inclusions that coexist with an immiscible carbonate liquid and the compositions of the quenched carbonate liquid reported by Mitchell (2009); however the presence of a CO_2-bearing vapor phase (Fig. 1d) could result in a bulk composition with higher CO_2 content. The salient point of Fig. 7a is that if the bulk composition of the system is in either the two liquid field or the two liquid plus vapor field then the composition of the silicate melt and carbonate liquid are fixed at a given pressure.

Fig. 7b shows the response of the two liquid solvus to changes in pressure, as determined experimentally by Brooker and Kjarsgaard (2011). At higher pressure, the two liquid field is broader and point "B" is in the one liquid field, in which case the OL bulk composition (silicate melt+carbonate liquid) would exist as a homogenous melt with ~12 wt% dissolved CO_2. High temperatures at depths of magma generation and earlier in the evolutionary history of the magma would also promote one liquid conditions (Brooker and Kjarsgaard, 2011). Upon decompression due to magma ascent, the two liquid solvus intersects the bulk composition and the magma exsolves a carbonate liquid, represented by the quenched carbonate inclusions of Mitchell (2009). As the magma continues to rise and decompress, the bulk composition enters the one liquid+vapor field, in which case the silicate melt is no longer buffered by the carbonate liquid and can lose CO_2 to the vapor phase. This is reflected in the OL matrix

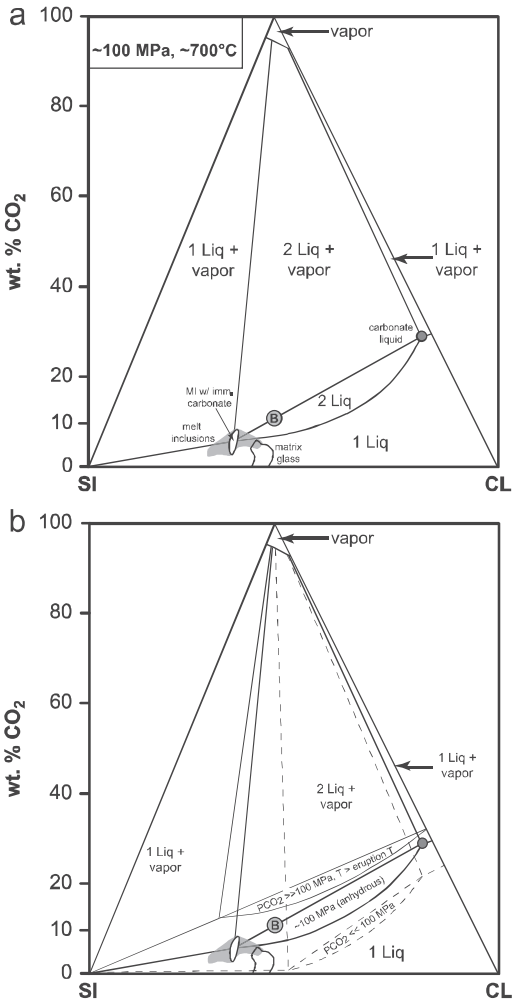

Fig. 7. (a) The two-liquid solvus plotted in CO_2 space for constant pressure and temperature (~100 MPa, 2.6 to 3.9 wt% H_2O, and ~700 °C; Kjarsgaard et al., 1995) along the projection plane SI–CL in Fig. 4 (after Brooker and Kjarsgaard, 2011; see their Fig. 9). The compositional fields for silicate melt inclusions, silicate melt inclusions with immiscible carbonate, matrix glass, and carbonate liquid (from Fig. 4) are plotted against the measured CO_2 content for the silicate glasses. The CO_2 content of the carbonate liquid was not analyzed by Mitchell (2009) and thus the deficits from 100% in analytical totals were used to estimate the CO_2 content. The bulk composition ("B") is depicted on the tie line between the coexisting silicate and carbonate liquids, but may fall at higher CO_2 conditions if a CO_2-bearing vapor phase was present. The position of the CO_2 apex is determined by projecting a vertical line through the bulk composition to 100% CO_2. The two-liquid solvus corresponds to ~100 MPa and ~700 °C for Oldoinyo Lengai compositions (Brooker and Kjarsgaard, 2011; Kjarsgaard et al., 1995). The matrix glass field extends to ~0 wt% CO_2 due to degassing of CO_2 at low pressure (see and Fig. 4 and Section 4.1). (b) The two-liquid solvus plotted schematically in CO_2 space for variable pressure (after Brooker and Kjarsgaard, 2011). The 100 Mpa 700 °C solvus is the same as that in (a). At conditions early in the evolutionary history of the system (i.e. high PCO_2 and high temperature) the bulk composition probably lay in the one-liquid field because increasing pressure displaces the two-liquid solvus towards the CO_2 apex and increasing temperature results in contraction of the two-liquid field (see schematic solvus labeled "$P \gg 100$ Mpa, T > eruption T"; after Brooker and Kjarsgaard, 2011). Ascent, decompression and cooling of the system results in intersection of the two-liquid field with the bulk composition ("~100 Mpa" solvus). As pressure decreases and the solvus migrates towards the field labeled "$P \ll 100$ MPa" the bulk composition first passes through the 2 liquid+vapor field, which would result in CO_2 gas exsolution from the system. Further decrease in pressure results in the bulk composition passing into the 1 liquid+vapor field resulting in matrix glass (which was quenched during eruption at low pressure) that has degassed most of its CO_2 (Fig. 4) and silicate melt that was no longer buffered by the carbonate liquid (Fig. 4 inset).

glasses, which display a wide range in CO_2 concentrations extending to degassed and highly peralkaline compositions.

Fig. 7a is based on the compositions of coexisting silicate glass and quenched carbonate liquid in inclusions from the 2007–2008 eruptive products and the two liquid solvus determined experimentally at 100 MPa for compositions of OL starting material containing 2.6–3.9 wt% H_2O (Kjarsgaard et al., 1995). Brooker and Kjarsgaard (2011) show that H_2O (and other volatiles) present in the vapor phase dilute CO_2, resulting in PCO_2 less than total P. The water-rich nature of OL melts is demonstrated for the first time in this study, and the behavior of water in the system could have important consequences for natrocarbonatite genesis. In a hydrous system, with PCO_2 less than P_{total} due to the presence or predominance of H_2O in the vapor phase, immiscible silicate and carbonate liquids could coexist at significantly higher pressures than previously determined. The commonly held assumption that OL magmas are anhydrous is based on the observation that natrocarbonatite lavas have low water content.

4.4.2. *Carbonate fluid evolution due to decompression and H_2O degassing*

There are few studies that have investigated water solubility in carbonatites due to experimental complexities, however Keppler (2003) found that water is highly soluble in carbonatite liquids, that solubility is strongly pressure dependent, and is given by the empirical relationship:

$$W = 0.4675P^{0.635} \quad (1)$$

where W is the solubility of H_2O in wt% and P is pressure in MPa. For example, at 200 MPa the experimental Na–Ca–Mg carbonate melt was water saturated at 13 wt% H_2O, whereas at 50 MPa it was saturated at ~6 wt% water. This is a reasonable result because water solubility would be expected to increase with pressure. Thus for the pressure range estimated from H_2O concentrations (30–300 MPa; minimum estimates) in silicate melt inclusions, an immiscible water-saturated carbonate liquid could contain 4.1–17.5 wt% H_2O, and the H_2O content of the carbonate liquid would depend on the initial H_2O concentration of the silicate melt and the partitioning behavior of H_2O between silicate melt and carbonate liquid.

Koster van Groos (1990) conducted a study on phase relationships in the binary system Na_2CO_3–H_2O at 100–925 °C and 40–370 MPa. Anhydrous Na_2CO_3 melts at 851 °C at 1 atm and anhydrous melting temperature increases with pressure. The natrocarbonatites at OL erupt at the surface as a liquid (with phenocrysts) at temperatures in the range of 550–650 °C and are relatively dry (~0.5 wt% H_2O; Keller and Spettel, 1995), illustrating that the pure Na_2CO_3 system is not directly comparable to the natural OL carbonatite. Vapor saturated melting temperature of $Na_2CO_3+H_2O$ decreases with pressure to about 600 °C at 100 MPa. However, the results of the study of Koster van Groos (1990) illustrate that $Na_2CO_3+H_2O$ can exist as a supercritical fluid at crustal pressures. For example, at 200 MPa and 700 °C a mixture of 45% Na_2CO_3 and 55% H_2O is a single supercritical fluid but at 100 MPa the same composition exists as a liquid composed of ~60% Na_2CO_3 and ~40% H_2O and a vapor phase that is ~95% H_2O and ~5% CO_2. The liquid+vapor field expands with decreasing pressure such that the liquid becomes less hydrous (20% H_2O at 50 MPa and 900 °C), consistent with the observation that erupting OL natrocarbonatites have low water content, and that H_2O solubility in carbonate liquids decreases with pressure, resulting in H_2O degassing. Similarly, carbonate liquids can also lose CO_2 to a vapor phase due to depression of the two liquid solvus in CO_2 space (Fig. 7b).

4.5. *Conceptual model for the eruptive cyclicity*

OL has a cyclical eruptive history, alternating between prolonged effusive natrocarbonatite eruptions and short-lived explosive nephelinite events (Dawson et al., 1992; Keller et al., 2010;

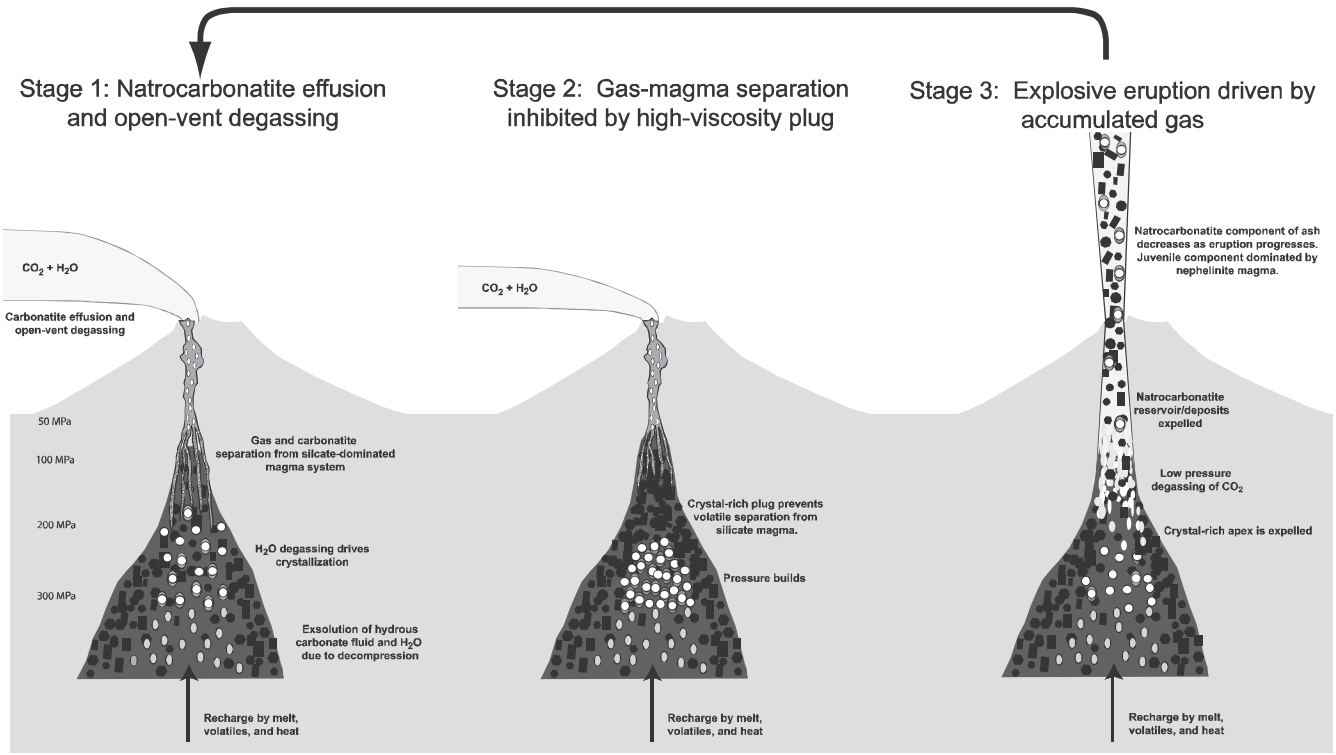

Fig. 8. Conceptual model for the cyclical eruptive behavior at OL. *Stage 1*: Effusive natrocarbonatite eruption and open-vent degassing is allowed because low viscosity and low density carbonate liquids and H_2O+CO_2 gas can separate from the nephelinite magma chamber. Recharge of melt, volatiles, and heat causes ascent of the silicate magma through the crust. Decompression results in exsolution of carbonate liquid and H_2O+CO_2 gas. Loss of water from the melt drives crystallization. *Stage 2*: Decompression, water loss, and crystallization result in high viscosity crystal-rich magma at the apex of the silicate magma system. Volatiles exsolved from deeper melt accumulate and cause overpressure. *Stage 3*: Explosive eruption occurs, expelling the crystal-rich apex and the overlying carbonatite reservoir (including previously emplaced natrocarbonatite) to produce mixed nephelinite+carbonatite ash. Once the mixed portion of the magma system is erupted, the ash becomes dominantly nephelinitic in composition. Once the crystal-rich apex of the magma system is expelled, natrocarbonatite effusion resumes (arrow).

Mitchell and Dawson, 2007). The samples of this study are most likely from the paroxysmal nephelinitic eruptions in early 2008 and provide insight into the explosive behavior. Here we present a conceptual model of the magmatic system, synthesizing models presented in the literature (Dawson, 1998; Keller et al., 2010; Kjarsgaard et al., 1995; Mattsson and Reusser, 2010; Mitchell, 2009; Mitchell and Dawson, 2012; Petibon et al., 1998; Pyle et al., 1991) with additions and modifications based on interpretation of the data in this study.

Volatiles, namely H_2O and CO_2, play a crucial role in the evolution and behavior of the magmatic system at OL. During effusive carbonatite periods (Fig. 8, stage 1), low viscosity and low density carbonate liquids exsolve from the nephelinite magma and are able to separate from the silicate magma chamber (e.g. Petibon et al., 1998), which makes up 98–75% of the total magma mass (e.g. Pyle et al., 1991). Voluminous gas emissions composed mostly of H_2O and CO_2 that are ultimately derived from decompression of silicate magmas occur during these open-vent periods (Brantley and Koepenick, 1995; Oppenheimer et al., 2002). We envision that the underlying nephelinite magma reservoir is replenished at depth by heat, volatiles, and melt, driving continuous rise of a complex and diverse magma column of crystallizing nephelinite melts, exsolution of hydrous carbonate liquid and $H_2O > CO_2$ gas (these could exist as a supercritical fluid at depth), depleting the silicate melt in H_2O and driving crystallization (Fig. 6b), whereas its CO_2 content is buffered by the presence of carbonate liquid (Figs. 4 and 7). Low density carbonate liquid is able to separate from its host and percolate up through the overlying magma column. Crystallization reduces the ratio of melt:crystals, allowing continual exsolution of carbonate liquid at buffered peralkalinity and dissolved CO_2 (Fig. 6). The low density carbonate liquid is able to separate from the nephelinite magma and ascend, resulting in decompression and H_2O degassing, to erupt at the surface as anhydrous natrocarbonatite (Section 4.4.2).

A fundamental change occurs when the system enters explosive episodes (Fig. 8, stage 2). The melt inclusion data show that the system is rich in volatiles, and that H_2O degassing takes place continuously through the evolution of melt. The nephelinitic source of volatiles provides the most likely cause of the explosivity. High degrees of crystallization driven by H_2O degassing results in increasing bulk magma viscosity, which inhibits gas separation from the silicate portion of the magma chamber (Fig. 8 stage 2). Overpressure in the silicate magma chamber causes the onset of the explosive eruption, expelling the upper natrocarbonatite reservoir and the mixed portion of the magma system (Fig. 8 stage 3) to produce mixed natrocarbonatite+nephelinite ash during the early phases of the eruption (Fig. 2; Keller et al., 2010; Mattsson and Reusser, 2010; Mitchell and Dawson, 2007). Decompression of the silicate magma chamber and expulsion of the overlying carbonatite portion of the magma chamber allows the silicate magma to continue evolving by rapid crystallization in response to decompression beyond carbonate liquid buffered conditions, either because the carbonate liquid had been expelled, or due to disequilibrium conditions (Brooker and Kjarsgaard, 2011), allowing the silicate melt to attain peralkalinity >5 and to degas CO_2 at low pressure (Dawson, 1998; Kjarsgaard et al., 1995), which may have contributed to the explosivity. The later eruptive deposits are dominated by combeite–wollastonite nephelinitic magmatic products (Keller et al., 2010; Mitchell and Dawson, 2012) because the upper portions of the magma system containing accumulated

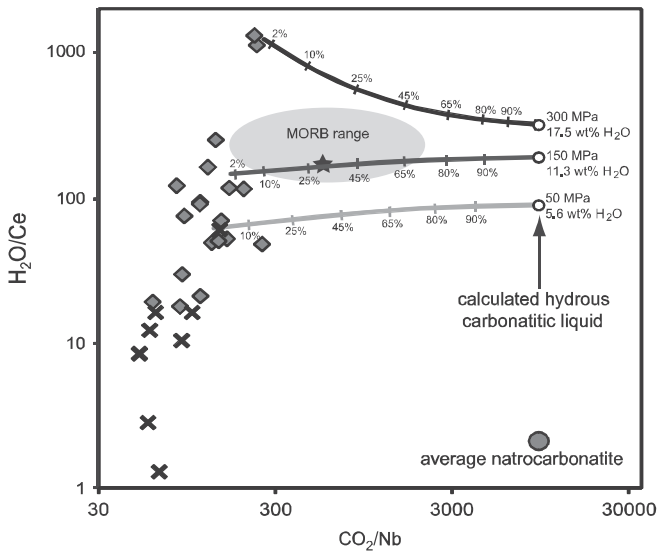

Fig. 9. H_2O/Ce versus CO_2/Nb showing the field for MORB from Cartigny et al. (2008), melt inclusions and matrix glass from the 2007–2008 eruption, and natrocarbonatite lava (the average composition of natrocarbonatite lavas erupted between 1988 and 2007; from Keller et al., 2010). Though the silicate melt inclusions are CO_2-rich, their CO_2/Nb ratios are less than MORB. The star indicates the composition of "Popping Rock", which is considered to be a pristine undegassed MORB sample. Also shown are calculated compositions of hydrous carbonate liquid at pressures determined from the H_2O content of the silicate melt inclusions, and mixing lines between hydrous carbonate liquid (the precursor to natrocarbonatite) and nephelinite melt inclusions. Carbonatite and silicate melts probably coexist in the magma system in a proportion of between 2 and 22 wt% carbonatite to 98–78 wt% silicate magma (Pyle et al., 1991). Therefore, the bulk magmatic system should fall on a mixing line between nephelinite melt inclusions and co-existing carbonate liquid at values between 2% and 22% (addition of carbonatite to silicate melt), indicating that a mantle source with high CO_2/Nb is not required.

carbonatite and mixed carbonatite+nephelinite were expelled during the early eruption (Fig. 2). Once the high viscosity crystal-rich nephelinite magma at the apex of the plumbing system has been explosively expelled, quiescent degassing and natrocarbonatite effusion resumes (Fig. 8 stage 1).

4.6. Nature of the mantle source

OL is one of the largest sources of volcanic CO_2 gas emissions globally, representing 2–3% of the estimated subaerial CO_2 flux (Brantley and Koepenick, 1995), and produces silicate glasses with the highest dissolved CO_2 measured to date. A fundamental issue related to the genesis of this carbon-rich system is the nature of the mantle source. Carbonatitic and hydrous metasomatic fluids are often invoked to explain trace element and radiogenic isotope characteristics of lithospheric xenoliths and erupted lavas (e.g. Aulbach et al., 2011), yet carbon-rich magmas can be produced from depleted mantle sources by low degrees of partial melting (e.g. Eggler, 1989).

Fig. 9 shows a plot of H_2O/Ce versus CO_2/Nb for the upper mantle as sampled by MORB, silicate melt inclusions and matrix glass from OL (this study), the average composition of recent natrocarbonatite lavas, and the modeled composition of hydrous carbonate liquid at pressure. Significantly, the melt inclusions and matrix glasses have lower CO_2/Nb ratios than the MORB range. The element pairs H_2O/Ce and CO_2/Nb have similar solid-melt partition coefficients and are minimally fractionated by melting or crystallization (e.g. Cartigny et al., 2008; Kingsley et al., 2002; Saal et al., 2002). However, exsolution of volatiles will decrease these ratios dramatically because neither Ce nor Nb is volatile. Fig. 9 shows that although melt inclusions from OL are extremely CO_2-rich (Table 1, Fig. 3), they have lower CO_2/Nb ratios than primitive melts derived from MORB mantle (Cartigny et al., 2008). Melt inclusions with the highest H_2O/Ce and CO_2/Nb are least evolved, as evidenced by low La and Ce, whereas the highly evolved matrix glass has low H_2O/Ce and CO_2/Nb. This relationship reflects H_2O and CO_2 loss due to volatile exsolution in conjunction with enrichment of Ce and Nb by crystallization. The steep slope of the nephelinite trend in Fig. 9 indicates that H_2O (rather than CO_2) was preferentially lost from the nephelinite melt, which is supported by high H_2O/CO_2 in gas emissions from OL measured by open-path Fourier transform infrared spectroscopy (Oppenheimer et al., 2002), as well as in our gas samples (full compositions to be presented elsewhere).

In comparison to melt inclusions or MORB, the natrocarbonatite lavas have high CO_2/Nb, and low H_2O/Ce (data from Keller et al., 2010). However, H_2O solubility increases dramatically in carbonate liquids with increasing pressure (Keppler, 2003). Pressures calculated from the H_2O content of silicate melt inclusions were used to estimate the H_2O content of the corresponding carbonate liquid (from Eq. (1)) over a reasonable pressure range (Kjarsgaard et al., 1995, Petibon et al., 1998). Radiogenic isotope and experimental studies suggest that natrocarbonatite originates by immiscible liquid "unmixing" of 2–25% carbonate liquid from nephelinite melt (e.g. Kjarsgaard et al., 1995; Pyle et al., 1991; Williams et al., 1986). The bulk liquid composition of the magma system should therefore fall on a mixing line between silicate melt and coexisting carbonate liquid. Mixing between the silicate melt inclusions and calculated hydrous carbonate liquid (Fig. 9) pass close to and through the field for MORB. The CO_2/Nb ratios for the magma system at reasonable mixtures of silicate and carbonate (i.e. $<25\%$ carbonate liquid) does not exceed the range observed in MORB. Our data indicate that an unusually carbon-rich mantle source is not required for any of the magmas erupted at OL. This model does not consider the gas phase, however a key piece of evidence in this regard is that the $CO_2/^3He$ of pristine gas samples from OL overlap with MORB (Fischer et al., 2009). Therefore, two completely independent volatile-based approaches (melt inclusions and gas samples) are consistent with a MORB-like CO_2 concentration in the mantle source region.

It is important to note that the magmas at OL are highly enriched in incompatible elements (in terms of whole rock and matrix glass compositions), have low MgO contents, and are therefore considered highly evolved. Even the least evolved melt inclusions cannot represent primary parental melts because they have low MgO contents. However, the lowest La, Ce, and Nb concentrations in the silicate melt (35 ppm, 50 ppm, and 100 ppm, respectively) are only slightly elevated outside of the MORB range (~1–20 ppm La, ~4–40 ppm Ce and ~1–40 ppm Nb; Cartigny et al., 2008). This observation highlights the long-standing problem in identifying primary parental magmas for the OL magmatic products (e.g. Klaudius and Keller, 2006; Mitchell and Dawson, 2012; Peterson, 1989; Peterson and Kjarsgaard, 1995), which is beyond the scope of this study but is an important issue that requires further investigation.

5. Summary and conclusions

The nephelinitic melt inclusions from the 2007–2008 explosive eruption of OL contain 2.7 wt% to 8.7 wt% CO_2, representing the highest CO_2 concentrations measured in natural silicate glasses to date, and 0.7 wt% to 10.1 wt% H_2O, indicating that water is an important component of the OL magma system. Whereas the glasses have exceptionally high CO_2 content, their CO_2/Nb ratios are lower than that in MORB, indicating that a carbon-rich mantle source is not required for generation of OL

magmas. We attribute the explosivity of the 2007–2008 eruption to the volatile-rich nature of the nephelinite melt. Degassing of water occurs over the range in melt inclusion compositions and carbonate liquids (precursors to natrocarbonatite lavas) exsolved from the silicate melt would contain up to 20 wt% H_2O at the highest H_2O-saturated pressures calculated for the silicate melt inclusions (300 MPa). Loss of water from the nephelinite melt is associated with incompatible element enrichment, suggesting that crystallization was driven by raising of the liquidus due to H_2O degassing.

We present a conceptual model for the eruptive cyclicity at OL in which magma ascent drives exsolution of hydrous carbonate liquids and H_2O-dominated gas. H_2O loss results in crystallization and increased bulk magma viscosity, which impedes gas separation from the silicate magma chamber and results in explosive expulsion of the crystal-rich apex of the nephelinite plumbing system, as well as the overlying mixed carbonatite+nephelinite upper magma reservoir. Once the crystal rich plug is expelled, quiescent degassing and natrocarbonatite effusion resume.

Acknowledgments

Funding was provided by NSF Grant EAR0827352 and the National Geographic Society (TPF), and a NASA Earth and Space Science student fellowship to JMdM. We acknowledge NSF support for the Arizona State University National SIMS Facility (EAR-0948878). We express deep gratitude to people of Engare Sero village, who were hospitable, allowed access to the volcano, and provided logistical support. We would like to acknowledge COSTECH for the 2009 research permit and support of scientists from the University of Dar Es Salaam. We thank Mike Spilde, Lynda Williams, Adrian Brearley, Stephan Schuth, and Nicole Thomas for analytical support. We would like to express our gratitude to Bruce Kjarsgaard, Tim Elliot (editor) and an anonymous reviewer whose comments and suggestions greatly improved this paper. We also acknowledge two anonymous reviewers who reviewed a previous version of this paper. TF thanks Bernard Marty and Pete Burnard for introducing him to Lengai in 2005.

Appendix A. Supporting information

Supplementary data associated with this article can be found in the online version at http://dx.doi.org/10.1016/j.epsl.2012.11.006.

References

Aulbach, S., Rudnick, R.L., McDonough, W.F., 2011. Evolution of the lithospheric mantle beneath the East African Rift in Tanzania and its potential signatures in rift magmas. Geol. Soc. Am. Spec. Pap. 478, 105–125.

Behrens, H., Misiti, V., Freda, C., Vetere, F., Botcharnikov, R.E., Scarlato, P., 2009. Solubility of H_2O and CO_2 in ultrapotassic melts at 1200 and 1250 °C and pressure from 50 to 500 MPa. Am. Mineral. 94, 105–120.

Brantley, S.L., Koepenick, K.W., 1995. Measured carbon-dioxide emissions from Oldoinyo-Lengai and the skewed distribution of passive volcanic fluxes. Geology 23, 933–936.

Brooker, R.A., Kjarsgaard, B.A., 2011. Silicate–Carbonate liquid immiscibility and phase relations in the system SiO_2–Na_2O–Al_2O_3–CaO–CO_2 at 0.1–0.25 GPa with applications to carbonatite genesis. J. Petrol. 52, 1281–1305.

Brooker, R.A., Sparks, R.S.J., Kavanagh, J.L., Field, M., 2011. The volatile content of hypabyssal kimberlite magmas: some constraints from experiments on natural rock compositions. Bull. Volcanol. 73, 959–981.

Cartigny, P., Pineau, F., Aubaud, C., Javoy, M., 2008. Towards a consistent mantle carbon flux estimate: insights from volatile systematics (H_2O/Ce, δD, CO_2/Nb) in the North Atlantic mantle (14°N and 34°N). Earth Planet. Sci. Lett. 265, 672–685.

Dawson, J.B., 1998. Peralkaline nephelinite–natrocarbonatite relationship at Oldoinyo Lengai, Tanzania. J. Petrol. 39, 2077–2094.

Dawson, J.B., Keller, J., Nyamweru, C., 1995. Historic and recent eruptive activity of Oldoinyo Lengai. In: Bell, K., Keller, J. (Eds.), Carbonatite Volcanism: Oldoinyo Lengai and the Petrogenesis of Carbonatites. IAVCEI Proceedings in Volcanology, Springer-Verlag, Berlin, pp. 70–86.

Dawson, J.B., Smith, J.V., Steele, I.M., 1992. 1966 Ash eruption of the carbonatite volcano Oldoinyo Lengai: mineralogy of lapilli and mixing of silicate and carbonatite magmas. Mineral. Mag. 56, 1–16.

Eggler, D.H., 1989. Carbonatites, primary melts, and mantle dynamics. In: Bell, K. (Ed.), Carbonatites: Genesis and Evolution. Unwin Hyman, London, pp. 561–579.

Fischer, T.P., Burnard, P., Marty, B., Hilton, D.R., Furi, E., Palhol, F., Sharp, Z.D., Mangasini, F., 2009. Upper-mantle volatile chemistry at Oldoinyo Lengai volcano and the origin of carbonatites. Nature 459, 77–80.

Guzmics, T., Mitchell, R.H., Szabo, C., Berkesi, M., Milke, R., Abart, R., 2011. Carbonatite melt inclusions in coexisting magnetite, apatite and monticellite in Kerimasi calciocarbonatite, Tanzania: melt evolution and petrogenesis. Contrib. Mineral. Petrol. 161, 177–196.

Hamilton, D.L., Bedson, P., Esson, J., 1989. The behavior of trace elements in the evolution of carbonatites. In: Bell, K. (Ed.), Carbonatites - Genesis and Evolution. Unwin Hyman, London, pp. 405–427.

Keller, J., Klaudius, J., Kervyn, M., Ernst, G.G.J., Mattsson, H.B., 2010. Fundamental changes in the activity of the natrocarbonatite volcano Oldoinyo Lengai, Tanzania. Bull. Volcanol. 72, 893–912.

Keller, J., Spettel, B., 1995. The trace element composition and petrogenesis of natrocarbonatites. In: Bell, K., Keller, J. (Eds.), Carbonatite Volcanism: Oldoinyo Lengai and the Petrogenesis of Natrocarbonatites. IAVCEI Proceedings in Volcanology, Springer-Verlag, Berlin, pp. 70–86.

Keller, J., Zaitsev, A.N., Wiedenmann, D., 2006. Primary magmas at Oldoinyo Lengai: the role of olivine melilitites. Lithos 91, 150–172.

Keppler, H., 2003. Water solubility in carbonatite melts. Am. Mineral. 88, 1822–1824.

Kervyn, M., Ernst, G.G.J., Keller, J., Vaughan, R.G., Klaudius, J., Pradal, E., Belton, F., Mattsson, H.B., Mbede, E., Jacobs, P., 2010. Fundamental changes in the activity of the natrocarbonatite volcano Oldoinyo Lengai, Tanzania. Bull. Volcanol. 72, 913–931.

King, P.L., Holloway, J.R., 2002. CO_2 solubility and speciation in intermediate (andesitic) melts: the role of H_2O and composition. Geochim. Cosmochim. Acta 66, 1627–1640.

Kingsley, R.H., Schilling, J.G., Dixon, J.E., Swart, P., Poreda, R., Simons, K., 2002. D/H ratios in basalt glasses from the Salas y Gomez mantle plume interacting with the East Pacific Rise: water from old D-rich recycled crust or primordial water from the lower mantle? art. no. 1025. Geochem. Geophys. Geosys. 3, 1025 1010.1029/2001GC000199.

Kjarsgaard, B.A., Hamilton, D.L., Peterson, T.D., 1995. Peralkaline nepheline/carbonatite liquid immiscibility: comparison of phase compositions in experiments and natural lavas from Oldoinyo Lengai. In: Bell, K., Keller, J. (Eds.), Carbonatite Volcanism: Oldoinyo Lengai and the Petrogenesis of Natrocarbonatites. Springer-Verlag, Berlin, pp. 163–190.

Klaudius, J., Keller, J., 2006. Peralkaline silicate lavas at Oldoinyo Lengai, Tanzania. Lithos 91, 173–190.

Koster Van Groos, A.F.K., 1990. High-pressure DTA study of the upper 3-phase region in the system Na_2CO_3–H_2O. Am. Mineral 75, 667–675.

Mattsson, H.B., Reusser, E., 2010. Mineralogical and geochemical characterization of ashes from an early phase of the explosive September 2007 eruption of Oldoinyo Lengai (Tanzania). J. Afr. Earth Sci 58, 752–763.

Mitchell, R.H., 2005. Carbonatites and carbonatites and carbonatites. Can. Mineral. 43, 2049–2068.

Mitchell, R.H., 2009. Peralkaline nephelinite–natrocarbonatite immiscibility and carbonatite assimilation at Oldoinyo Lengai, Tanzania. Contrib. Mineral. Petrol. 158, 589–598.

Mitchell, R.H., Dawson, J.B., 2007. The 24th September 2007 ash eruption of the carbonatite volcano Oldoinyo Lengai, Tanzania: mineralogy of the ash and implications for a new hybrid magma type. Mineral. Mag. 71, 483–492.

Mitchell, R.H., Dawson, J.B., 2012. Carbonate–silicate immiscibility and extremely peralkaline silicate glasses from Nasira cone and recent eruptions at Oldoinyo Lengai Volcano, Tanzania. Lithos , http://dx.doi.org/10.1016/j.lithos.2012.01.006.

Moore, G., 2008. Interpreting H_2O and CO_2 contents in melt inclusions: constraints from solubility experiments and modeling. In: Putirka, K.D., Tepley, F.J. (Eds.), Minerals, Inclusions and Volcanic Processes. Mineralogical Society of America, Chantilly, pp. 333–361.

Nielsen, T.F.D., Solovova, I.P., Veksler, I.V., 1997. Parental melts of melilitolite and origin of alkaline carbonatite: evidence from crystallised melt inclusions, Gardiner complex. Contrib. Mineral. Petrol. 126, 331–344.

Oppenheimer, C., Burton, M.R., Durieux, J., Pyle, D.M., 2002. Open-path Fourier Transform spectroscopy of gas emissions from Oldoinyo Lengai volcano, Tanzania. Opt. Laser Eng. 37, 203–214.

Peterson, T.D., 1989. Peralkaline Nephelinites.2. Low-Pressure Fractionation and the Hypersodic Lavas of Oldoinyo-Lengai. Contrib. Mineral. Petrol. 102, 336–346.

Peterson, T.D., Kjarsgaard, B.A., 1995. What are the parental magmas at Oldoinyo Lengai? In: Bell, K., Keller, J. (Eds.), Carbonatite Volcanism: Oldoinyo Lengai and the Petrogenesis of Natrocarbonatites. IAVCEI Proceedings in Volcanology, Springer-Verlag, Berlin, pp. 100–112.

Petibon, C.M., 1999. The genesis of natrocarbonatites: constraints from experimental petrology and trace element partitioning. Memorial University of Newfoundland, St. John's.

Petibon, C.M., Kjarsgaard, B.A., Jenner, G.A., Jackson, S.E., 1998. Phase relationships of a silicate-bearing natrocarbonatite from Oldoinyo Lengai at 20 and 100 MPa. J. Petrol. 39, 2137–2151.

Pyle, D.M., Dawson, J.B., Ivanovich, M., 1991. Short-lived decay series disequilibria in the natrocarbonatite lavas of Oldoinyo Lengai, Tanzania—constraints on the timing of magma genesis. Earth Planet. Sci. Lett. 105, 378–396.

Russell, J.K., Porritt, L.A., Lavallée, Y., Dingwell, D.B., 2012. Kimberlite ascent by assimilation-fuelled buoyancy. Nature 481, 352–356.

Saal, A.E., Hauri, E.H., Langmuir, C.H., Perfit, M.R., 2002. Vapour undersaturation in primitive mid-ocean-ridge basalt and the volatile content of Earth's upper mantle. Nature 419, 451–455.

Safonov, O.G., Kamenetsky, V.S., Perchuk, L.L., 2011. Links between carbonatite and kimberlite melts in chloride–carbonate–silicate systems: experiments and application to natural assemblages. J. Petrol. 52, 1307–1331.

Schmidt, B.C., Behrens, H., 2008. Water solubility in phonolite melts: influence of melt composition and temperature. Chem. Geol. 256, 259–268.

Sharygin, V.V., Kamenetsky, V.S., Zaitsev, A.N., Kamenetsky, M.B., 2012. Silicate–natrocarbonatite liquid immiscibility in 1917 eruption combeite–wollastonite nephelinite, Oldoinyo Lengai Volcano, Tanzania: melt inclusion study. Lithos , http://dx.doi.org/10.1016/j.lithos.2012.01.021.

Sokolov, S.V., Veksler, I.V., Senin, V.G., 1999. Alkalis in carbonatite magmas: new evidence from melt inclusions. Petrology 7, 602–609.

Sparks, R.S.J., 2003. Dynamics of magma degassing. In: Oppenheimer, C., Pyle, D.M., Barclay, J. (Eds.), Volcanic Degassing. The Geological Society, London, pp. 5–22.

Veksler, I.V., Petibon, C., Jenner, G.A., Dorfman, A.M., Dingwell, D.B., 1998. Trace element partitioning in immiscible silicate–carbonate liquid systems: an initial experimental study using a centrifuge autoclave. J. Petrol. 39, 2095–2104.

Vigouroux, N., Wallace, P.J., Kent, A.J.R., 2008. Volatiles in high-K magmas from the western Trans-Mexican volcanic belt: evidence for fluid fluxing and extreme enrichment of the mantle wedge by subduction processes. J. Petrol 49, 1589–1618.

Watson, E.B., Green, T.H., 1981. Apatite liquid partition-coefficients for the rare-earth elements and strontium. Earth Planet. Sci. Lett. 56, 405–421.

Webster, J.D., Mandeville, C.W., 2007. Fluid immiscibility in volcanic environments. Rev. Mineral. Geochem. 65, 313–362.

Williams, R.W., Gill, J.B., Bruland, K.W., 1986. Ra–Th disequilibria systematics—timescale of carbonatite magma formation at Oldoinyo Lengai volcano, Tanzania. Geochim. Cosmochim. Acta 50, 1249–1259.

Wyllie, P.J., Huang, W.L., 1975. Peridotite, kimberlite, and carbonatite explained in system CaO–MgO–SiO_2–CO_2. Geology 3, 621–624.